Inter-reader agreement of ^{18}F-FDG PET/CT for the quantification of carotid artery plaque inflammation

Kjersti Johnsrud[1,2*], Therese Seierstad[3], David Russell[2,4], Mona-Elisabeth Revheim[1,2]

[1] Department of Nuclear Medicine, Division of Radiology and Nuclear Medicine, Oslo University Hospital, Oslo, Norway

[2] Institute of Clinical Medicine, University of Oslo, Oslo, Norway

[3] Department for Research and Development, Division of Radiology and Nuclear Medicine, Oslo University Hospital, Oslo, Norway

[4] Department of Neurology, Oslo University Hospital, Oslo, Norway

[*]Corresponding author

E-mail: kjersti@slogum.no (KJ)

Abstract

Background: A significant proportion of ischemic strokes are caused by emboli from unstable atherosclerotic carotid artery plaques with inflammation being a key feature of plaque instability and stroke risk. Positron emission tomography (PET) depicting the uptake of 2-deoxy-2-(^{18}F)-fluoro-D-glucose **(**^{18}F-FDG) in carotid artery plaques is a promising technique to quantify plaque inflammation. A consensus on the methodology for plaque localization and quantification of inflammation by ^{18}F-FDG PET/computed tomography (CT) in atherosclerosis has not been established. High inter-reader agreement is essential if ^{18}F-FDG PET/CT is to be used as a clinical tool for the assessment of unstable plaques and stroke risk. The aim of our study was to assess the inter-reader variability of different methods for quantification of ^{18}F-FDG uptake in carotid atherosclerotic plaques with a separate CT angiography (CTA) providing anatomical guidance.

Methods and results: Forty-three patients with carotid artery stenosis ≥70% underwent ^{18}F-FDG PET/CT. Two independent readers separately delineated the plaque in all axial PET slices containing the atherosclerotic plaque and the maximum standardized uptake value (SUV_{max}) from each slice was measured. Uptake values with and without background correction were calculated. Intraclass correlation coefficients were highest for uncorrected uptake values (0.97-0.98) followed by those background corrected by subtraction (0.89-0.94) and lowest for those background corrected by division (0.74-0.79). There was a significant difference between the two readers definition of plaque extension, but this did not affect the inter-reader agreement of the uptake parameters.

Conclusions: Quantification methods without background correction have the highest inter-reader agreement for ^{18}F-FDG PET of carotid artery plaque inflammation. The use of the single highest uptake value (max SUV_{max}) from the plaque will facilitate the method's clinical utility in stroke prevention.

Introduction

Ischemic strokes caused by thromboembolism from an unstable atherosclerotic plaque in the carotid artery can be prevented by carotid endarterectomy (CEA) [1-3]. Patients are selected for CEA based on the degree of carotid artery stenosis and presence or absence of cerebral ischemic symptoms. In recent years it has become increasingly clear that the degree of stenosis alone is not the best predictor of stroke risk. This has led to the concept of the 'unstable plaque' describing carotid plaques that carry high risk of stroke irrespective of the degree of artery stenosis and increased focus on factors that destabilize the plaque. Inflammation plays a key role in the development of an unstable plaque [4-6].

Positron emission tomography (PET) imaging of atherosclerosis has been rapidly evolving since the first reports of 2-deoxy-2-(^{18}F)-fluoro-D-glucose (^{18}F-FDG) uptake localized to the inflammatory macrophage rich areas in carotid artery plaques [7]. The goal of the imaging technique is to detect carotid plaques that are at high risk of rupture and therefore carry high risk of stroke. ^{18}F-FDG PET for the detection of unstable plaques is not in clinical use [8], partly due to lack of feasible PET protocols and consensus regarding imaging procedure, method for ^{18}F-FDG uptake quantification and assessment of stroke risk, although several recommendations exist [9, 10]. PET is an imaging modality with limited anatomical information, and it might therefore be challenging to define the vessel-segment-of-interest. Computed tomography angiography (CTA) is often used together with ^{18}F-FDG PET when assessing patients with carotid artery stenosis, but selection of the plaque area for uptake measurements varies [11-13]. A requirement for introducing a diagnostic method into clinical routine is high inter-reader agreement. Inter-reader agreement has been studied for a few selected uptake parameters with generalized vascular inflammation [14, 15] and in patients with symptomatic carotid stenosis [12, 13], but to our knowledge no study has compared inter-reader agreement for different quantification methods.

The aim of this study was to assess inter-reader variability of different methods used for quantification of ^{18}F-FDG uptake at PET/CT of carotid artery plaques.

Materials and methods

Study population

The study cohort consisted of forty-three patients with ultrasound-confirmed atherosclerosis with internal carotid artery stenosis ≥70% according to consensus criteria of the Society of Radiologists in Ultrasound [16]. Patient characteristics are summarized in Table 1. There were 30 men (66 ± 9 years) and 13 women (67 ± 8 years) with a mean age of 66.2 years. The study protocol conformed with the ethical guidelines of the 1975 Declaration of Helsinki and was approved by the Norwegian Regional Committee for Medical and Health Research Ethics. Written informed consent was obtained from all patients prior to study inclusion.

Table 1. Patient characteristics (n = 43) *

Age, years; mean ± SD	66.2 ± 8.4
Sex, male; n (%)	30 (69.8)
Blood glucose, mmol·L^{-1}; mean ± SD (range)	6.8 ± 2.2 (4.9 - 14.9)
Bodyweight, kg; mean ± SD (range)	82.4 ± 15 (55 - 110)
Body mass index, kg/m^2; mean ± SD (range)	27.5 ± 4.5 (19.9 - 34.8)

*The patient material is included in previously published studies [17, 18].

^{18}F-FDG PET/CT examination

After a minimum of six hours fasting the patients were injected with 5 MBq/kg ^{18}F-FDG and blood glucose, weight, and height were recorded. After approximately 90 minutes a two-bed position PET/CT from the base of the skull to the aortic arch was performed with 15 minutes per bed position using a hybrid PET/CT scanner (Siemens Biograph 64, Siemens Medical Systems, Erlangen, Germany). The PET images were acquired with a 256x256 matrix and the images were reconstructed to two millimetre thick slices, with four iterations/eight subsets ordered subset expectation–maximization (OSEM) algorithm and Gaussian post-reconstruction filter with 3.5 mm full width half maximum (FWHM). In addition to a non-contrast CT for attenuation correction a CTA with contrast filling of the arteries (minimum 40ml Iomeron (iodine 350mg/ml; Bracco Imaging S.P.A, Milan, Italy) or Visipaque (iodine 320mg/ml); GE Healthcare, Chicago, USA) was acquired immediately after the PET when still lying in the scanner for 16 of the 43 patients. For 24 patients CTA was performed at other radiologic departments. For three patients no CTA was available when the PET images were analysed.

Image analyses and ^{18}F-FDG quantification

The images were assessed with Hybrid Viewer 2.0 software (Hermes Medical Solutions AB, Stockholm, Sweden). Two experienced nuclear medicine senior consultants independently evaluated the ^{18}F-FDG PET/CT examinations. The two readers (R1 and R2) did not undergo any joint training before assessing the images, but they agreed on how to perform the analyses. The instructions were to use the CTA as guide for drawing the region of interests (ROIs) on the fused slices (PET and non-contrast CT). The plaque was defined as vessel wall thickening and a lumen contrast-filling defect on CTA [11]. The ROIs were drawn

around the entire vessel wall and lumen on all plaque-containing axial PET slices (Fig 1). For patients without CTA available, the plaque was defined as vessel wall with calcification and fat deposits in the level of the carotid bifurcation. Uptake in structures close to the plaque (e.g. lymph nodes, paravertebral muscles or salivary glands) that could falsify the plaque uptake values were excluded from the ROI. The number of plaque-containing slices for each patient was recorded. The pixel values in the PET images were converted into SUV and normalized to lean body mass [19]. SUV_{max} in all plaque containing ROIs were recorded. Background blood pool activity was obtained from four ROIs placed in the lumen of the jugular vein away from structures with ^{18}F-FDG uptake but preferably in the same craniocaudal level as the plaque. The background was calculated as the mean of the SUV_{mean} in these four ROIs. Different measures of ^{18}F-FDG uptake were calculated (Table 2) as previously described in detail [17]. Blood background corrected values were calculated as the ^{18}F-FDG uptake values divided by the mean blood pool activity (TBR) and subtraction of the blood pool activity from the ^{18}F-FDG uptake values (corrected SUV (cSUV)).

Fig 1. Region of interest. On each plaque-containing axial slice a region of interest (ROI) was drawn manually around the entire vessel wall including the plaque and the lumen. A (fused PET/non-contrast CT) and B (PET) show increased uptake (arrow) in the plaque in the right internal carotid artery. C shows how the plaque location on contrast enhanced CT (low attenuation plaque with thin contrast filled lumen in the centre) guides the actual drawing of the ROI (green dotted line) on the fused PET/non-contrast CT (D).

142 **Table 2. Plaque ^{18}F-FDG uptake measures.**

Uptake measure	Description
max SUV_{max}	the single highest SUV_{max}
mean SUV_{max}	mean of all plaque SUV_{max}
MDS3*	mean SUV_{max} of the three contiguous slices centered on the slice with the highest SUV_{max}
MDS5*	mean SUV_{max} of the five contiguous slices centered on the slice with the highest SUV_{max}
mean $SUV_{max}4$	mean SUV_{max} of the four slices with highest SUV_{max}

143 *MDS, most diseased segment

144

145 # Statistical analysis

146 The IBM SPSS Statistics software for Windows (version 25.0; IBM Corp., Armonk,
147 USA) was used for data analyses. Groups of paired data were compared using the Wilcoxon
148 signed rank test for non-normally distributed variables. Inter-reader agreement was calculated
149 using intraclass correlation coefficients (ICC's; model two-way random, type absolute
150 agreement). All statistical results were considered significant when $p < 0.05$. All uptake
151 values per patient can be found in a supplementary data file (S1 File).

152

153

154

155

156

157

158

159

Results

The different ^{18}F-FDG uptake values for the two readers are summarized in Table 3. Reader 2 identified significantly more slices as plaque containing (median; 10, range; 4-23) than reader 1 (median; 9, range; 3-18) (p = 0.001).

Table 3. ^{18}F-FDG uptake values and intraclass correlation coefficients between the two readers (n = 43 patients)

Quantification method	^{18}F-FDG uptake values			ICC
	Reader 1	Reader 2	*p*	
Max SUV_{max}	1.74 (1.18 - 2.66)	1.74 (1.20 - 2.66)	0.304	.979
Mean SUV_{max}	1.51 (1.11 - 2.28)	1.51 (1.06 - 2.15)	0.687	.973
MDS3	1.68 (1.17 - 2.51)	1.68 (1.19 - 2.51)	0.400	.978
MDS5	1.64 (1.15 - 2.32)	1.63 (1.17 - 2.45)	0.438	.972
Mean SUV_{max}4	1.68 (1.15 - 2.45)	1.68 (1.13 - 2.45)	0.060	.972
Background	0.87 (0.55 - 1.26)	0.89 (0.55 - 1.30)	0.245	.767
TBR max SUV_{max}	1.95 (1.34 - 3.07)	2.02 (1.34 - 2.68)	0.314	.792
TBR mean SUV_{max}	1.72 (1.16 - 2.59)	1.76 (1.25 - 2.37)	0.232	.741
TBR MDS3	1.87 (1.26 - 2,89)	1.97 (1.30 - 2.55)	0.296	.775
TBR MDS5	1.80 (1.22 - 2.79)	1.94 (1.24 - 2.53)	0.241	.769
TBR mean SUV_{max} 4	1.81 (1.26 - 2.82)	1.93 (1.31 - 2.61)	0.358	.758
cSUV max SUV_{max}	0.83 (0.42 - 1.79)	0.87 (0.38 - 1.67)	0.837	.944
cSUV mean SUV_{max}	0.68 (0.20 - 1.28)	0.68 (0.28 - 1.19)	0.435	.893
cSUV MDS3	0.80 (0.33 - 1.64)	0.79 (0.34 - 1.51)	0.769	.931
cSUV MDS5	0.75 (0.28 - 1.45)	0.76 (0.27 - 1.45)	0.595	.916
cSUV mean SUV_{max}4	0.74 (0.32 - 1.58)	0.77 (0.35 - 1.45)	0.975	.919

Data are given as median (range). *P*-value from Wilcoxon signed ranks test. SUV, standardized uptake value; MDS, most diseased segment; TBR, target-to-background ratio; cSUV, background subtracted SUV; ICC, intraclass correlation coefficient.

There were no differences in ^{18}F-FDG uptake between the two readers (Table 3). The ICC for the different ^{18}F-FDG quantification methods was highest for uncorrected SUVs (0.97-0.98) followed by cSUVs (0.89-0.94) and TBRs (0.74-0.79), and 0.77 for the

174 background blood pool (Table 3). The differences in the median for the uptake values
175 between the readers ranged from 0.00 and 0.01 for the uncorrected SUVs to 0.04-0.14 for
176 TBRs (0.14 for TBR MDS5). The difference for the background value was 0.02 (Table 3).
177 Fig 2 shows the differences in max SUV_{max} and mean SUV_{max} for individual patients
178 for the two readers without background correction (A and B), and the corresponding values
179 when the ^{18}F-FDG uptake is corrected for background blood pool by division (TBR; 2C and
180 2D) and by subtraction (cSUV; 2E and 2F). The difference in venous background is shown in
181 Fig 2G. The difference between the readers is highest for the uptake values corrected for
182 background blood pool by division (2C and 2D). and lowest for the uptake values without
183 background correction (2A and 2B).
184

185 **Fig 2. Inter-reader difference for the ^{18}F-FDG quantification methods.** Difference
186 between the readers (R2 minus R1, y-axis)) for the included patients (x-axis). Max SUV_{max}
187 (A), mean SUV_{max} (B), TBR max SUV_{max} (C), TBR mean SUV_{max} (D), cSUV max SUV_{max}
188 (E), cSUV mean SUV_{max} (F), and venous background (G).
189

190 # Discussion

191 In this study we found high inter-reader agreement between different methods for ^{18}F-
192 FDG uptake quantification of inflammation in high grade carotid artery stenosis. The inter-
193 reader agreement was highest for the methods without background correction. Two studies in
194 patients with carotid stenosis supports our finding that methods without correction for
195 background blood activity have higher inter-reader agreement than background corrected
196 values: Kwee et al. [12] reported an ICC of 0.61 for TBR mean SUV_{max} and 0.65 for TBR
197 max $SUV_{max,}$ and Marnane et al. [13] found an ICC of 0.99 for mean SUV_{max}.

198 In our study the highest ICC was found for max SUV_{max} (0.98). For the methods
199 without background blood pool correction only 12% of the max SUV_{max} and 14% of the mean
200 SUV_{max} measurements differed with more than ± 0.10 (Fig 2A, B). Patient number 42 is an
201 outlier with an inter-reader difference of 0.38. This is probably due to different delineations of
202 the plaque ROIs as this patient had high uptake in neighbouring muscle (Fig 3). Reader 1 can
203 have excluded more of the plaque ROIs to be sure to avoid spill-in activity than reader 2. The
204 problem with spill-in from neighbouring structures is due to the relatively low spatial
205 resolution of PET combined with unspecific uptake of ^{18}F-FDG.
206
207 **Fig 3. Spill-in activity.** Fused image of non-contrast CT and PET (A) and contrast enhanced
208 CT (B) show a plaque in the level of the right carotid bifurcation with low uptake but with
209 high uptake in nearby muscles. PET with normal intensity on the SUV scale (C) and PET with
210 high intensity on the SUV scale (D) show that ^{18}F-FDG uptake from nearby muscle activity
211 influences the ROI around the plaque (inserted picture at 4 to 5 o'clock position).
212
213 For the background corrected values, the difference was larger with 40% of TBR max
214 SUV_{max} and 30% of TBR mean SUV_{max} having a difference of ± 0.25 or more (Fig 2C, D). In
215 our previous study exploring ^{18}F-FDG-uptake in symptomatic versus asymptomatic patients
216 [18] the difference in median mean SUV_{max} between the groups was 0.32 (1.75 versus 1.43).
217 In two studies using TBR max SUV_{max} as uptake parameter the difference was found to be
218 0.19 and 0.29 [20, 21]. Thus, methods with reader difference of 0.25 prohibit differentiation
219 between symptomatic and asymptomatic patients.
220 We found an ICC for background blood pool activity of 0.77. This discordant
221 assessment of background blood pool activity introduces variation in TBR and cSUVs due to
222 methodology rather than biology. The background blood pool activity in our study was

obtained from four ROIs within the lumen of the jugular vein preferably in the same craniocaudal level as the plaque. The vena jugularis has a small diameter and it was often challenging to draw reproducible ROIs within the vein that excluded contribution from neighbouring structures. In a ^{18}F-FDG PET study of generalized vascular inflammation in which the background blood pool activity was obtained from eight ROIs in the jugular vein the ICC for TBR mean SUV_{max} of the carotid arteries was 0.94-0.96 [14]. This suggests that including data from more slices or from a larger vessel segment such as the vena cava superior or atria of the heart could have reduced the inter-reader variability of measuring the blood pool activity. In this study the two readers also had trained together by co-reading several pilot studies before they established an analysis protocol [14]. This is optimal for research studies, but hard to accomplish in larger trials where the readers often are located in different departments.

There is a large amount of studies that quantifies the ^{18}F-FDG uptake in the vessel wall of patients with suspected generalized vascular inflammation (atherosclerosis not necessarily confirmed by other imaging methods). Although our findings cannot automatically be generalized, one might question the need for background correction for these patients.

Reader 2 included significantly more plaque-containing slices than reader 1. This did not reduce the ICC of the ^{18}F-FDG measurements, supporting that the plaque slices with the highest uptake values all were included in both readers plaque area and that the number of slices included in the plaque area has minimal influence on mean SUV_{max}. Our interpretation of this finding is that the plaque inflammation we can detect with ^{18}F-FDG PET is homogeneously spread out, and also present in the extreme tails of the plaque. This was also one of our main findings when we explored associations between different ^{18}F-FDG uptake parameters and plaque inflammation at histopathology [17]. Furthermore, this is in

248 accordance with the study results from Kwee et al. [12] who found a strong correlation
249 between TBRs of ipsilateral symptomatic plaques and contralateral asymptomatic plaques and
250 supports the hypothesis that plaque inflammation is systemic to some extent.

251 A strength of our study is a relatively large patient population with a wide range of
252 uptake values (max SUV_{max} from 1.18 to 2.66) representing low to high plaque inflammatory
253 activity confirmed by histology [17].

254 In conclusion, our study confirms the reproducibility of quantification of ^{18}F-FDG
255 uptake in carotid artery plaques and supports the superiority of quantification methods that do
256 not include blood pool background**.** The ICC was highest for max SUV_{max} (the single highest
257 uptake value within the plaque) and thus, our suggestion is to further explore this parameter
258 for atherosclerosis imaging.

259

260 Supporting information

261 **S1 File.** SPSS file with individual ^{18}F-FDG uptake measurements.

262

263 Author Contributions

Contributor Role	Role Definition
Conceptualization	Kjersti Johnsrud, Therese Seierstad, David Russell, Mona-Elisabeth Revheim **Ideas; formulation or evolution of overarching research goals and aims.**

Data Curation	Kjersti Johnsrud **Management activities to annotate (produce metadata), scrub data and maintain research data (including software code, where it is necessary for interpreting the data itself) for initial use and later reuse.**
Formal Analysis	Kjersti Johnsrud, Therese Seierstad, Mona-Elisabeth Revheim **Application of statistical, mathematical, computational, or other formal techniques to analyze or synthesize study data.**
Funding Acquisition	David Russell **Acquisition of the financial support for the project leading to this publication.**
Investigation	Kjersti Johnsrud, Therese Seierstad, Mona-Elisabeth Revheim **Conducting a research and investigation process, specifically performing the experiments, or data/evidence collection.**
Methodology	Kjersti Johnsrud, Therese Seierstad, David Russell, Mona-Elisabeth Revheim **Development or design of methodology; creation of models**
Project Administration	David Russell **Management and coordination responsibility for the research activity planning and execution.**
Resources	David Russell, Therese Seierstad, Mona-Elisabeth Revheim **Provision of study materials, reagents, materials, patients, laboratory samples, animals, instrumentation, computing resources, or other analysis tools.**
Supervision	David Russell, Therese Seierstad, Mona-Elisabeth Revheim **Oversight and leadership responsibility for the research activity planning and execution, including mentorship external to the core team.**

Validation	Kjersti Johnsrud, Therese Seierstad, Mona-Elisabeth Revheim **Verification, whether as a part of the activity or separate, of the overall replication/reproducibility of results/experiments and other research outputs.**
Visualization	Kjersti Johnsrud, Therese Seierstad **Preparation, creation and/or presentation of the published work, specifically visualization/data presentation.**
Writing – Original Draft Preparation	Kjersti Johnsrud, Therese Seierstad, Mona-Elisabeth Revheim **Creation and/or presentation of the published work, specifically writing the initial draft (including substantive translation).**
Writing – Review & Editing	Kjersti Johnsrud, Therese Seierstad, David Russell, Mona-Elisabeth Revheim **Preparation, creation and/or presentation of the published work by those from the original research group, specifically critical review, commentary or revision – including pre- or post-publication stages.**

References

1. Gasecki AP, Eliasziw M, Ferguson GG, Hachinski V, Barnett HJ. Long-term prognosis and effect of endarterectomy in patients with symptomatic severe carotid stenosis and contralateral carotid stenosis or occlusion: results from NASCET. North American Symptomatic Carotid Endarterectomy Trial (NASCET) Group. Journal of neurosurgery. 1995;83(5):778-82.

2. Group ECSTCE. Randomised trial of endarterectomy for recently symptomatic carotid stenosis: final results of the MRC European Carotid Surgery Trial (ECST). Lancet. 1998;351(9113):1379-87.

3. Barnett HJ, Taylor DW, Eliasziw M, Fox AJ, Ferguson GG, Haynes RB, et al. Benefit of carotid endarterectomy in patients with symptomatic moderate or severe stenosis. North American Symptomatic Carotid Endarterectomy Trial Collaborators. The New England journal of medicine. 1998;339(20):1415-25.

4. Libby P. Inflammation in atherosclerosis. Nature. 2002;420(6917):868-74.

5. Stoll G, Bendszus M. Inflammation and atherosclerosis: novel insights into plaque formation and destabilization. Stroke. 2006;37(7):1923-32.

6. Jander S, Sitzer M, Schumann R, Schroeter M, Siebler M, Steinmetz H, et al. Inflammation in high-grade carotid stenosis: a possible role for macrophages and T cells in plaque destabilization. Stroke. 1998;29(8):1625-30.

7. Rudd JH, Warburton EA, Fryer TD, Jones HA, Clark JC, Antoun N, et al. Imaging atherosclerotic plaque inflammation with [18F]-fluorodeoxyglucose positron emission tomography. Circulation. 2002;105(23):2708-11.

8. Chowdhury MM, Tarkin JM, Evans NR, Le E, Warburton EA, Hayes PD, et al. (18)F-FDG Uptake on PET/CT in Symptomatic versus Asymptomatic Carotid Disease: a Meta-Analysis. European journal of vascular and endovascular surgery : the official journal of the European Society for Vascular Surgery. 2018;56(2):172-9.

9. Bucerius J, Hyafil F, Verberne HJ, Slart RH, Lindner O, Sciagra R, et al. Position paper of the Cardiovascular Committee of the European Association of Nuclear Medicine (EANM) on PET imaging of atherosclerosis. European journal of nuclear medicine and molecular imaging. 2016;43(4):780-92.

10. Huet P, Burg S, Le Guludec D, Hyafil F, Buvat I. Variability and uncertainty of 18F-FDG PET imaging protocols for assessing inflammation in atherosclerosis: suggestions for improvement. Journal of nuclear medicine : official publication, Society of Nuclear Medicine. 2015;56(4):552-9.

11. Graebe M, Borgwardt L, Hojgaard L, Sillesen H, Kjaer A. When to image carotid plaque inflammation with FDG PET/CT. Nuclear medicine communications. 2010;31(9):773-9.

12. Kwee RM, Truijman MT, Mess WH, Teule GJ, ter Berg JW, Franke CL, et al. Potential of integrated [18F] fluorodeoxyglucose positron-emission tomography/CT in identifying vulnerable carotid plaques. AJNR American journal of neuroradiology. 2011;32(5):950-4.

13. Marnane M, Merwick A, Sheehan OC, Hannon N, Foran P, Grant T, et al. Carotid plaque inflammation on 18F-fluorodeoxyglucose positron emission tomography predicts early stroke recurrence. Annals of neurology. 2012;71(5):709-18.

14. Rudd JH, Myers KS, Bansilal S, Machac J, Pinto CA, Tong C, et al. Atherosclerosis inflammation imaging with 18F-FDG PET: carotid, iliac, and femoral uptake reproducibility, quantification methods, and recommendations. Journal of nuclear medicine : official publication, Society of Nuclear Medicine. 2008;49(6):871-8.

15. Rudd JH, Myers KS, Bansilal S, Machac J, Rafique A, Farkouh M, et al. (18)Fluorodeoxyglucose positron emission tomography imaging of atherosclerotic plaque inflammation is highly reproducible: implications for atherosclerosis therapy trials. Journal of the American College of Cardiology. 2007;50(9):892-6.

16. Grant EG, Benson CB, Moneta GL, Alexandrov AV, Baker JD, Bluth EI, et al. Carotid artery stenosis: gray-scale and Doppler US diagnosis--Society of Radiologists in Ultrasound Consensus Conference. Radiology. 2003;229(2):340-6.

17. Johnsrud K, Skagen K, Seierstad T, Skjelland M, Russell D, Revheim ME. (18)F-FDG PET/CT for the quantification of inflammation in large carotid artery plaques. Journal of nuclear cardiology : official publication of the American Society of Nuclear Cardiology. 2019;26(3):883-93.

18. Skagen K, Johnsrud K, Evensen K, Scott H, Krohg-Sorensen K, Reier-Nilsen F, et al. Carotid plaque inflammation assessed with (18)F-FDG PET/CT is higher in symptomatic compared with asymptomatic patients. International journal of stroke : official journal of the International Stroke Society. 2015;10(5):730-6.

19. Boellaard R, Delgado-Bolton R, Oyen WJ, Giammarile F, Tatsch K, Eschner W, et al. FDG PET/CT: EANM procedure guidelines for tumour imaging: version 2.0. European journal of nuclear medicine and molecular imaging. 2015;42(2):328-54.

20. Muller HF, Viaccoz A, Fisch L, Bonvin C, Lovblad KO, Ratib O, et al. 18FDG-PET-CT: an imaging biomarker of high-risk carotid plaques. Correlation to symptoms and microembolic signals. Stroke. 2014;45(12):3561-6.

21. Tarkin JM, Joshi FR, Evans NR, Chowdhury MM, Figg NL, Shah AV, et al. Detection of Atherosclerotic Inflammation by (68)Ga-DOTATATE PET Compared to [(18)F]FDG PET Imaging. Journal of the American College of Cardiology. 2017;69(14):1774-91.

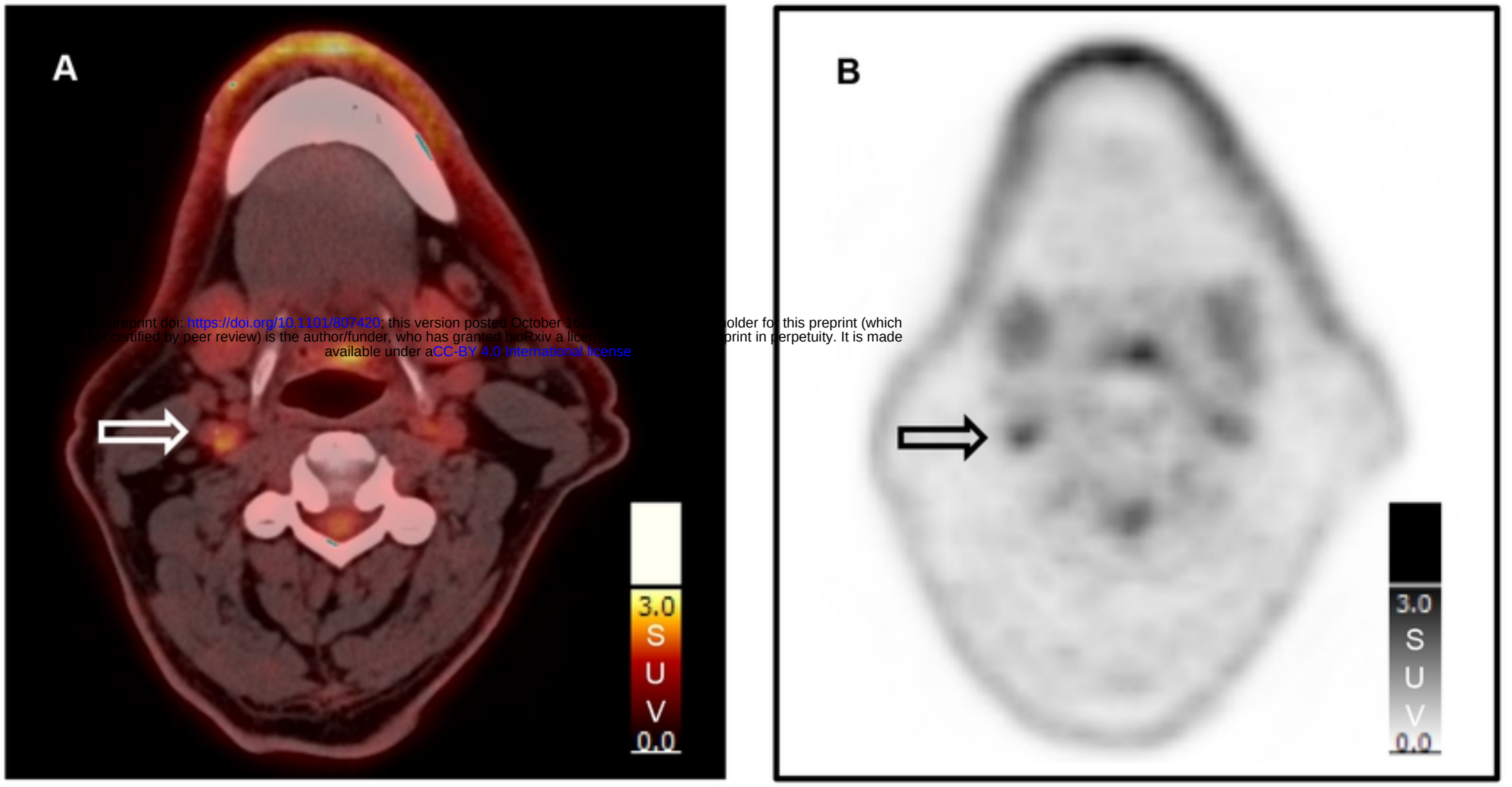

Fig1

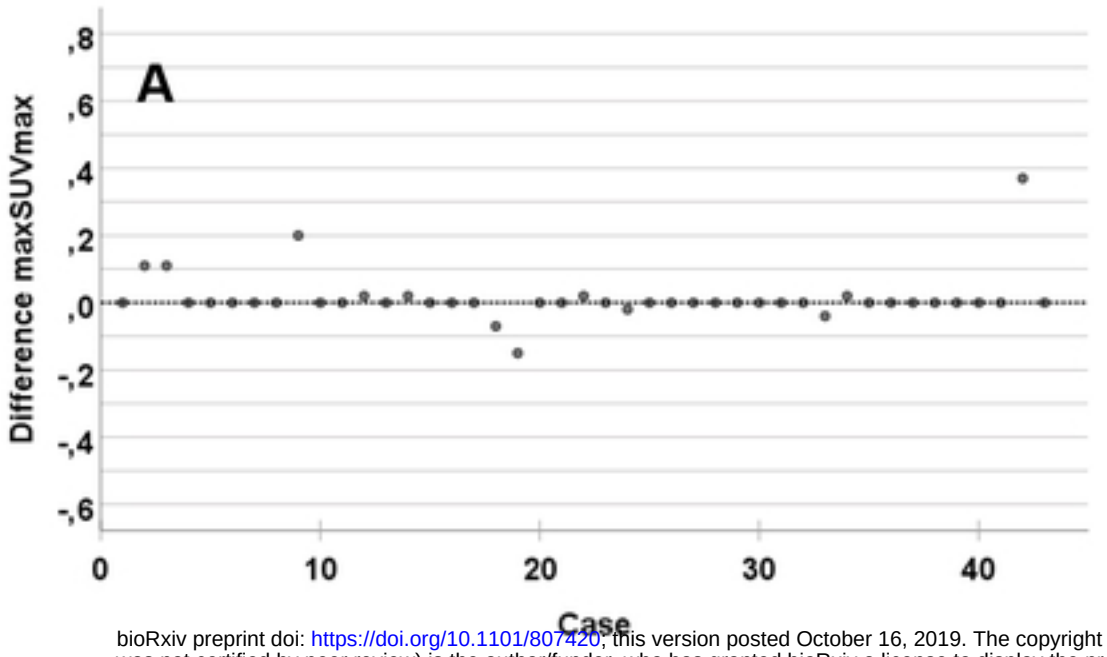

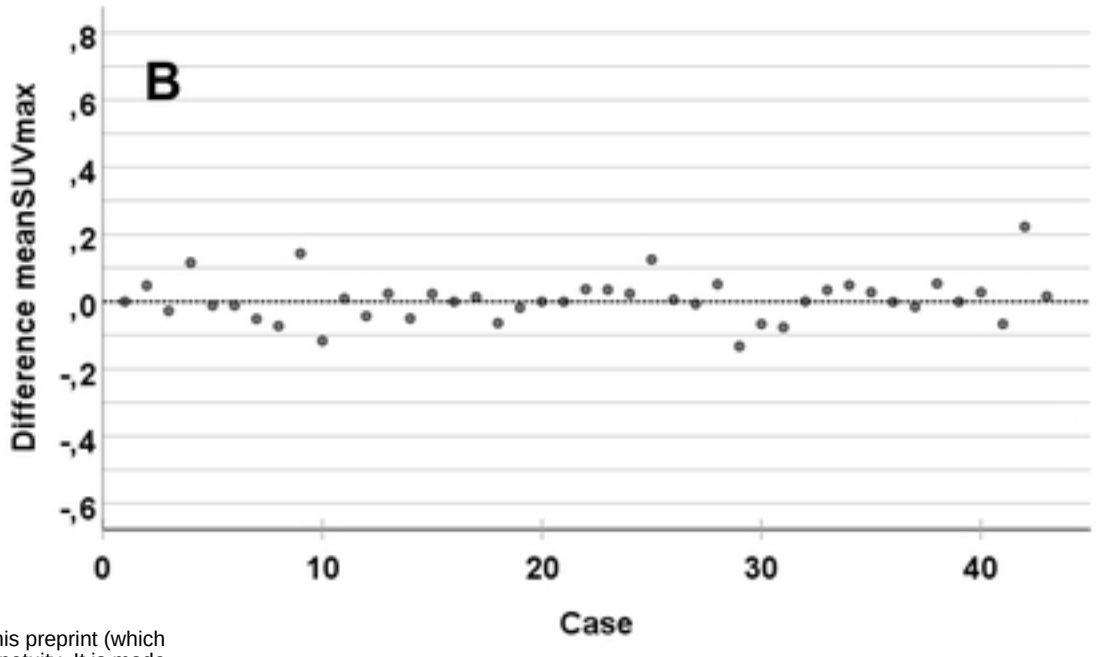

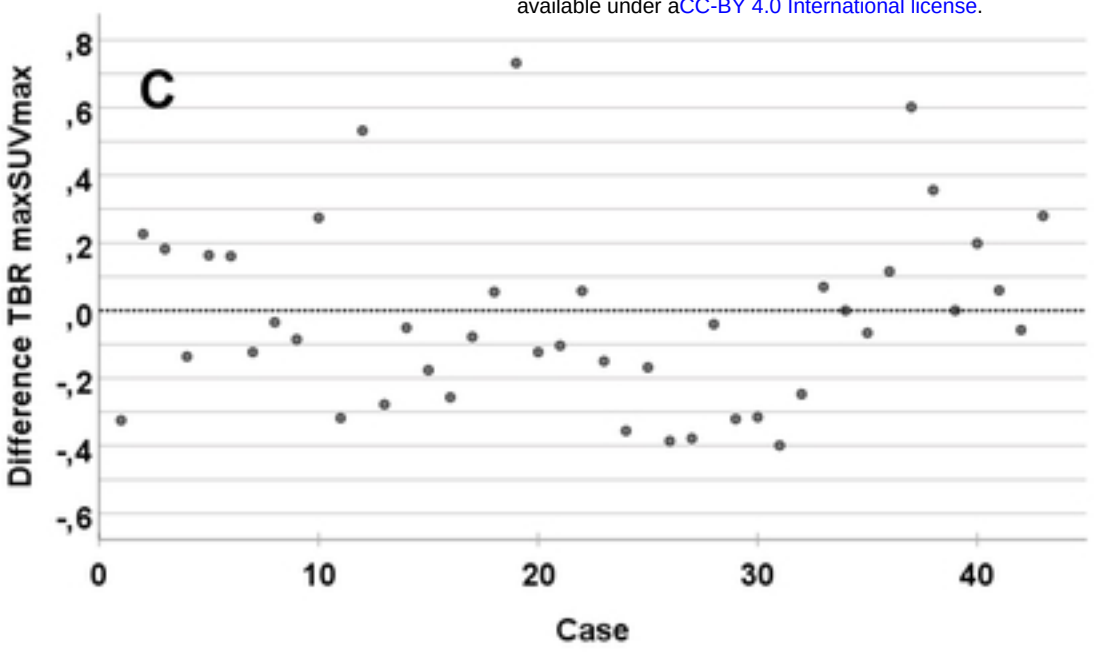

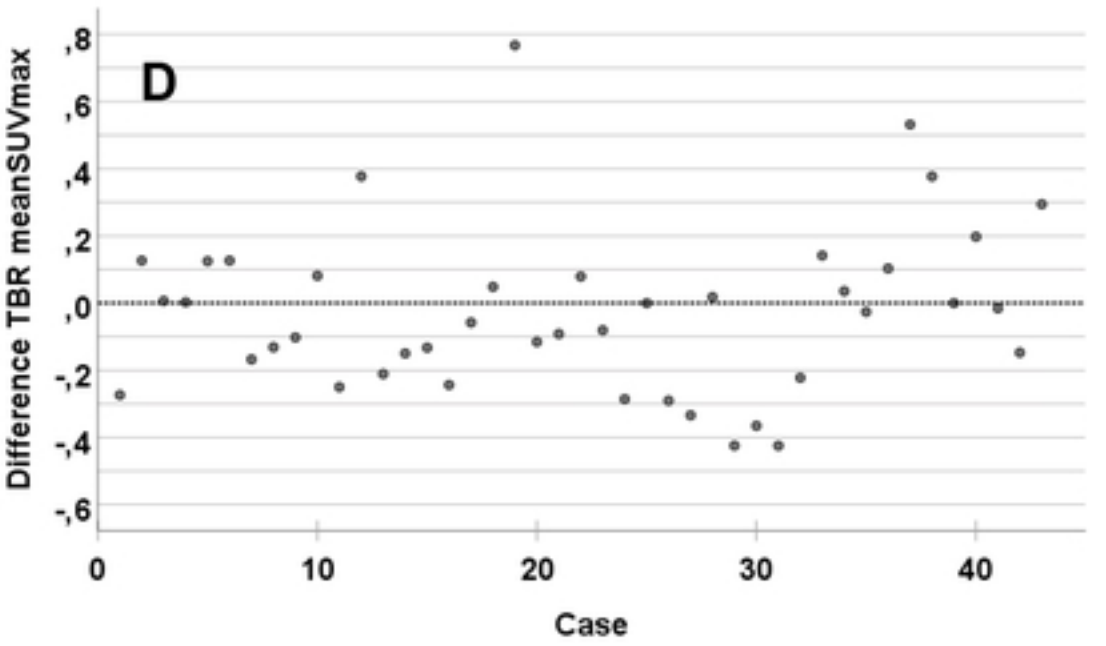

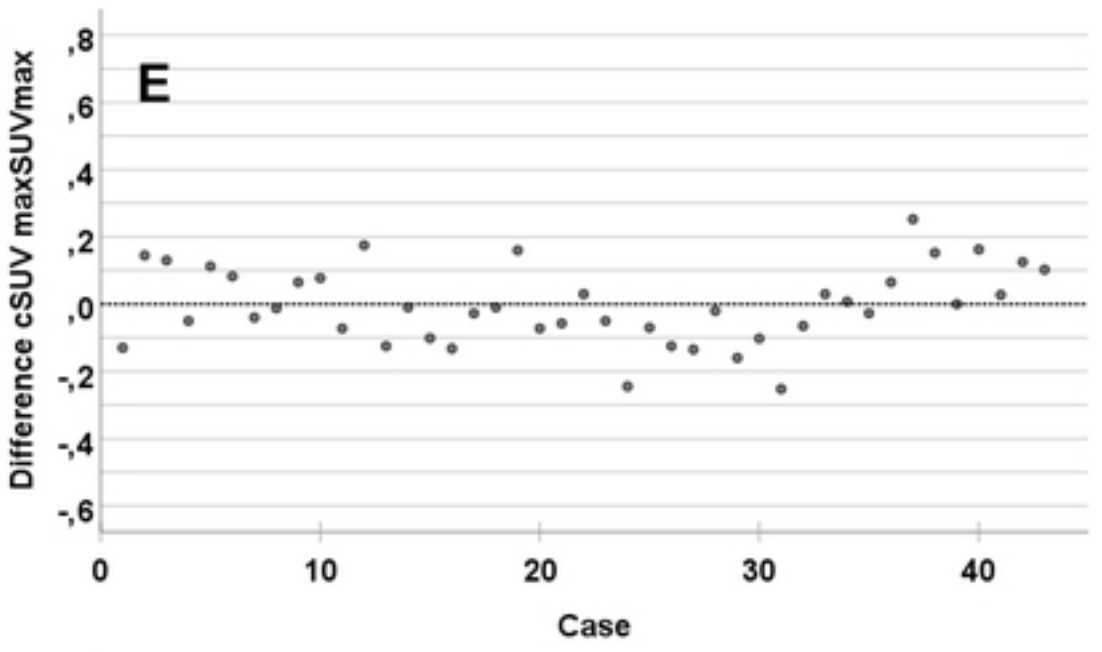

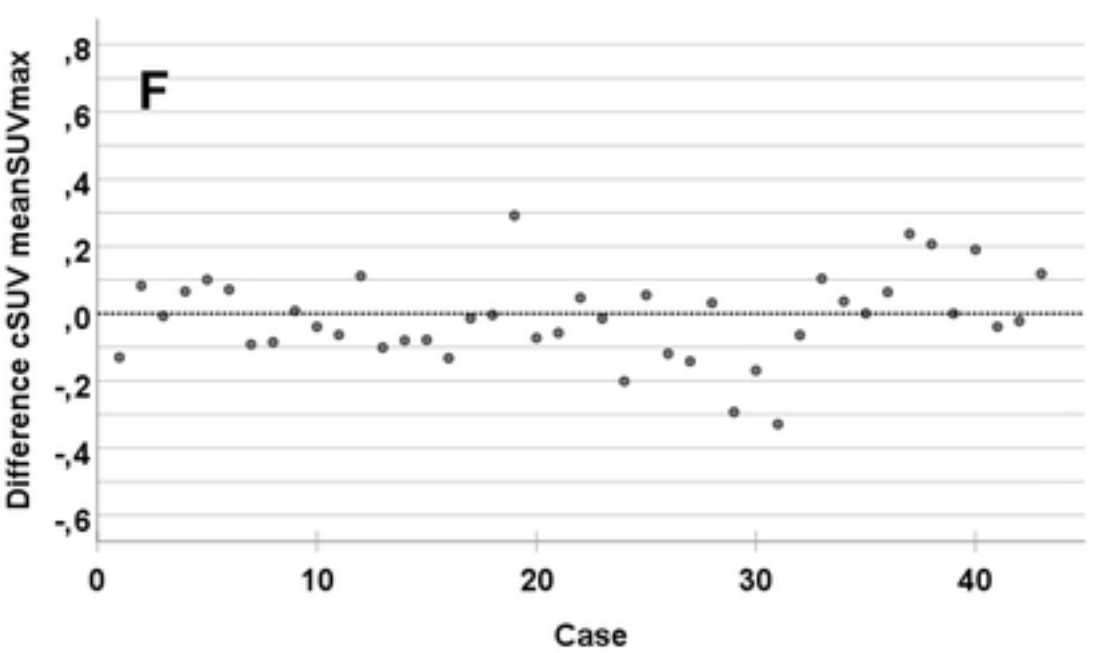

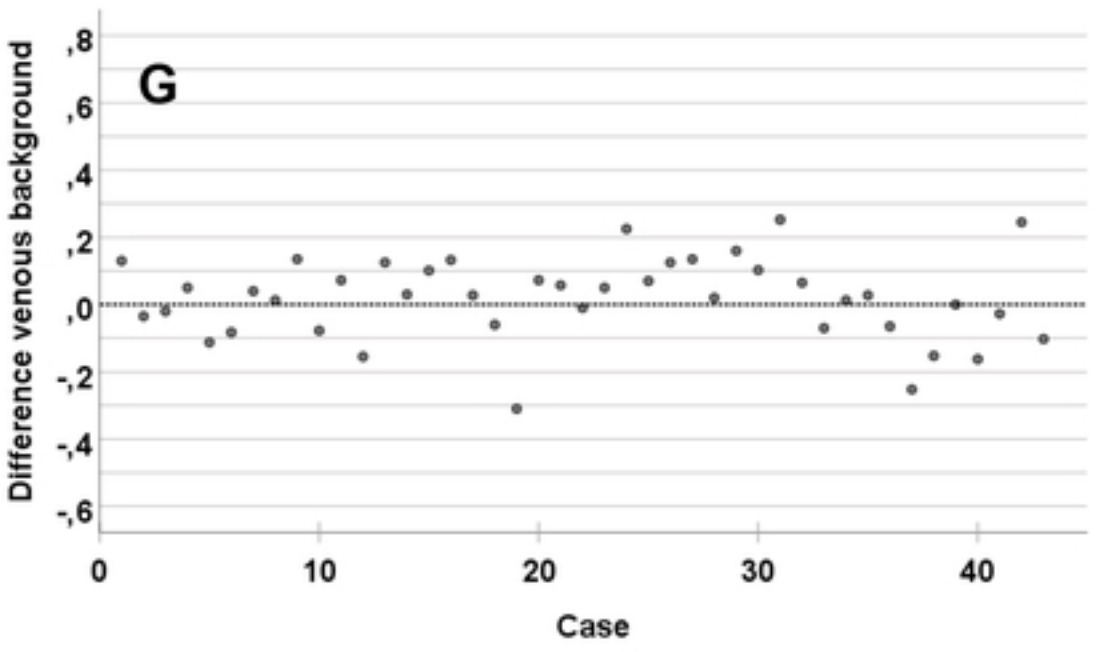

Fig2

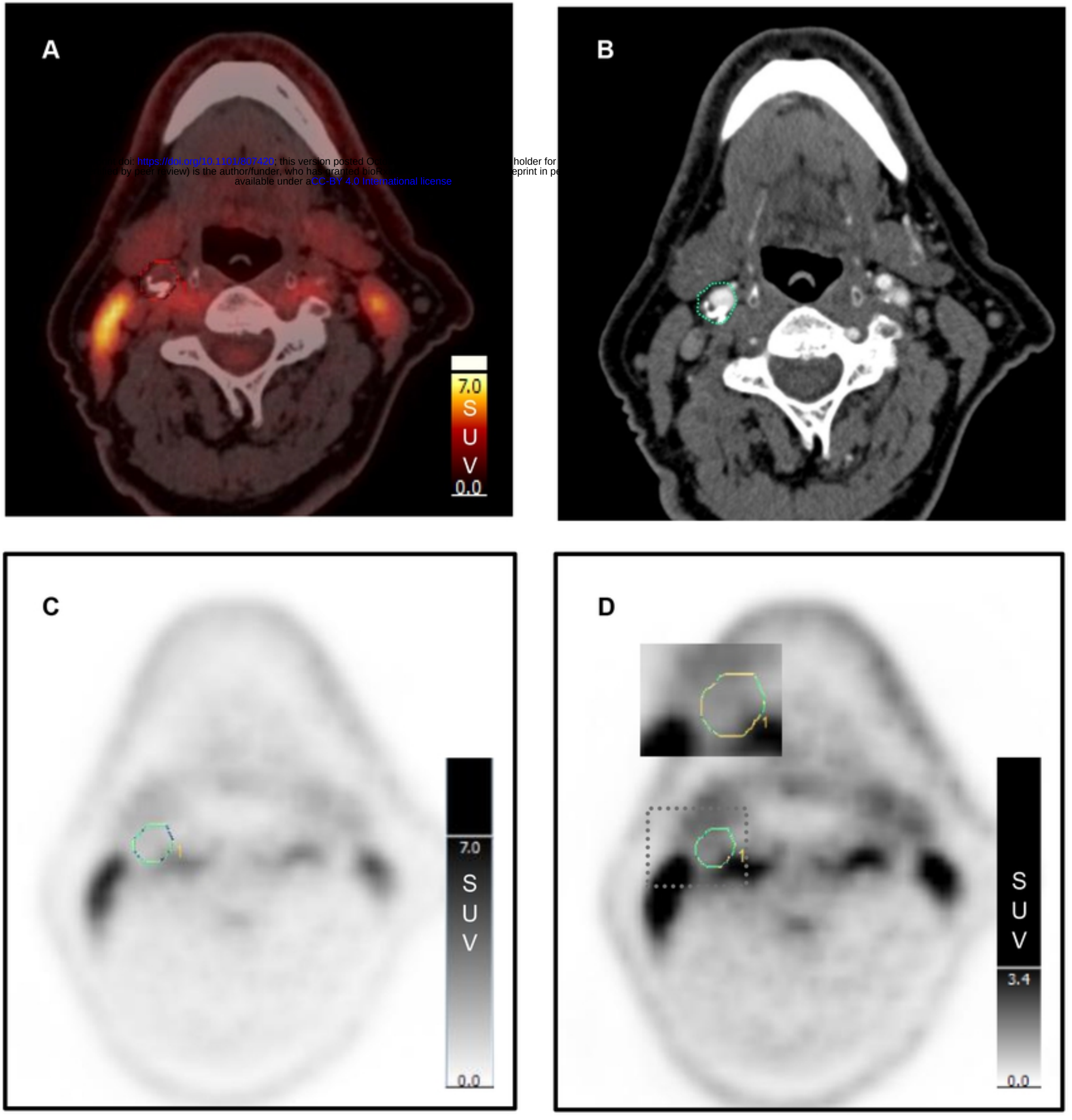

Fig3